Title: Investigation on the possible control of grain-size on development of 'mud-cracks': a preliminary experimental study of recent Gangetic alluvial samples, West Bengal, India

Authors: Soumyadip Banerjee[1,3], Abhik Kundu[1*], Patrick G. Eriksson[2], Subhajit Sinha[3]

Affiliations:

[1]Department of Geology, Asutosh College, 92 S.P. Mukherjee Road, Kolkata- 700026, West Bengal, India.
[2]Department of Geology, University of Pretoria, Pretoria 0002, South Africa.
[3]Department of Geology, University of Calcutta. 35, Ballygunge Circular Road, Kolkata- 700019, West Bengal, India.
*Corresponding author email ID:kundu.abhik@gmail.com,abhikgeology@asutoshcollege.in

Abstract

The so-called mud cracks, possibly the most common deformation feature in sediment, are evident in almost all dried-up exposed sediment surfaces. Several experimental attempts have so far been made to explain evolution of mud cracks. However, most of the experiments were carried out with bentonite clay or other artificial substances in controlled heating condition. Therefore, those experiments could not or were not performed to elucidate the control of grain-size on crack development although it has been observed that cracks develop in almost all types of soil. The present work is an attempt to understand the control of sediment grain-size in development and evolution of these cracks. This experimental study was carried out in near-natural condition. Sediment samples of three different grain-size fractions ranging from sub-sand size to very coarse sand size were used for the experiment. The ten-day long experiment with watering and drying of the samples under sunlight shows that the time gap between watering and appearance of cracks, smoothness of crack walls, number of cracks and also number of polygons with cracks as their arms are dependent on grain-size of the sediment.

Keywords: Mud crack formation, natural sediment, grain-size, air passage through sediment, incubation period of cracking, mud crack geometry.

1. Introduction

Mud cracks constitute a common group of sediment deformation structures which owe their origin to desiccation and shrinkage (Kindle 1917; Adams and Hanks 1964; Collinson and Thompson 1982; Weinberger 1999; Colina and Roux 2000; Kodikara et al. 2000; Nichols 2009; Peron et al. 2009; Gauthier et al. 2010; Reineck and Sing 2012; Goehring et al. 2015). Clay in sediment acts as a cohesive substance in presence of water (Partheniades 2009; Grabowski et al. 2011). Volume loss due to evaporation results in amalgamation of clay particles (Nichols 2009) causing a tensile stress, which if it exceeds the tensile strength of the soil causes formation of cracks (Weinberger 1999). Mud cracks are readily visible in the dry seasons, almost everywhere on the exposed surfaces of soil cover. The diversity in patterns and dimensions make their morphology vis-a-vis origin an interesting subject of study.

Experiment based explanations of origin of mud cracks are common in published literature (Kindle 1917; Corte and Higashi 1960; Groisman and Kaplan 1994; Zabat et al. 1997; Korneta 1998; Colina and Roux 2000; Shorlin, et al. 2000; Liang et al. 2003; Bhon et al. 2005; Vogel and Roth 2005; Peron et al. 2009; Goehring et al.

2010, 2013; Style et al. 2011). However, a thorough study of the existing literature on mud cracks reveals that most of the experiments were carried out with bentonite clay or with materials like starch, laponite and with montmorillonite under regulated and artificially heated conditions (Groisman and Kaplan 1994; Zabat et al. 1997; Korneta 1998; Colina and Roux 2000; Shorlin 2000; Liang et al. 2003; Bhon et al. 2005; Vogel and Roth 2005; Peron et al. 2009; Goehring et al. 2010, 2013; Style et al. 2011). Therefore, in each of these experiments the samples were homogeneous and would have behaved uniformly. Moreover, the artificially created ambience must have been distinctly different from the natural situations of crack generation and evolution.

These deficiencies of existing experimental works can be improved upon through further experiments with natural soil samples, with inherent physical heterogeneity, in a near natural ambience, as far as possible, in order to replicate and also to explain generation and evolution of mud cracks in the natural scenario. Moreover, the control of grain-size is not commented upon by any previous work though from field studies it is obvious that cracks form not only in mud (with clay-sized particles) but also in sandy soil and even in sediment with particles coarser than sand. Schieber (1998) points out that, sandstones (and sands) may also crack if they contain significant proportions of clay minerals, or if the sandstone bed had a microbial mat growing on its upper surface, to provide cohesiveness analogous to that provided by the clays (see also, Schieber et al. 2007 and references therein). The experiments as performed here exclude formation of microbial mats. The present work thus aims to understand the control of grain-size, one of the most important physical properties of soil, on morphology of cracks as well as the temporal evolution of crack patterns in a single natural wetting and drying phase.

2. Methodology:

2.1 Samples and Experiment

A wet lumpy sample from Gangetic alluvium was collected. The sample was dried in an oven (at 105°C-110°C for 24 hours; cf. Tan 2005). The oven dried sample was differentiated into three fractions: (i) fine gravel <grain-size ≥ coarse sand, (ii) grain-size = medium sand and (iii) grain-size ≤ fine sand, using an electrically operated gyratory sieve shaker fitted with ASTM calibrated sieves (ISO 14688-1:2002). Three separate sample blocks, each with dimensions of 24cm x 19cm x 3cm, were prepared in plastic trays of dimension of 24cm x 19cm x 4.5cm (**Figs. 1 a, b** and **c**); one was for coarse sand (henceforth addressed as sample 1), one for medium sand (henceforth addressed as sample 2), and the third for fine sand and finer grains (henceforth addressed as sample 3). Each sample was kept under natural temperature condition of the West Bengal summer (average temperature 34°C and humidity ~72% according to the Indian Meteorological Department, Government of India,

http://www.imd.gov.in). All the three samples were placed on a perfectly horizontal floor, tested by a double bubble spirit level. Water was sprinkled from approximately 30cm above the exposed surface of the sample block (Goehring 2010) through a hand held mist sprinkler in order to avoid displacement of grains at the top surfaces and resulting deformation. Water was added to each sample (Table 1) until the exposed soil-surface was below a 0.5cm water depth, in order to replicate the inundation that the soil undergoes in the monsoon times (**Fig. 1b**). This condition we considered as a state of super-saturation, as it is assumed that the water level can only rise above the top surface of the sample after filling all the available pore spaces. The volume of water required to achieve such state varies with samples (Table 1). Photographs were taken once every day for the entire period of the experiment, which was a ten-day span. Crack morphology, number of cracks and relative area occupied by cracks with respect to exposed surface area of the sample trays, as well as crack lengths were observed.

2.2 X-ray diffraction

The material from each of the three samples was also analysed for its mineralogy through X-ray diffraction. This was done in order to assess how mineralogy may have interacted with grain-size differences in forming cracks, crack patterns and their characteristics.

All the samples were dried at 60ºC for 10-12 hours before running through XRD. Selected samples were also analysed sequentially on air dried slides and then glycolated. The dried powdered (< 200 mesh) samples were taken in a sample holder and pressed with a glass slide (press mount method). All the samples were analyzed by a fully automated computerized X'pert PRO PANalytical XRD, using Cu-Kα radiation at the Department of Geological Sciences, Jadavpur University, Kolkata, India. The XRD was operated at 40 kV/30mA and the samples were scanned from 5º to 70º 2θ, at a running speed of 1º 2θ per minute. The diffraction patterns thus obtained were first interpreted by computer software and then checked manually. Semi-quantitative estimations of the relative concentrations of the constituent minerals were carried out on computer program and manually based on the peak area method (Biscaye 1965). The XRD patterns of whole samples were obtained following Brown and Brindley (1984).

3. Results and observations

3.1 XRD mineralogy

Taking the samples together, XRD analysis determined quartz as the dominant mineral, with lesser amounts of montmorillonite, polylithionite and lavendulan (**Figs. 2 a, b** and **c**). While quartz was present universally in all

the samples, montmorillonite was found only in the fine and medium sand samples (respectively samples 3 and 2), with polylithionite exclusive to sample 2, and lavendulan to sample 3.

3.2 Crack characteristics as observed in the three samples

A general observation from all the samples is that triple-junction crack patterns were developed from pore throats (cf, Baldwin 1974; Weinberger 1999) (**Figs. 3 a, b**) which formed during watering. Sample-wise observations are presented in the following subsections.

3.2.1 Sample 1 (fine gravel <grain-size ≥ coarse sand):

Cracks appeared in this sample on the 6thday after watering. Crack walls were rough. Propagation paths of the cracks were not straight. A total of nine triple junctions, with cracks mostly oriented at 120^{o} to each other, were formed out of which three remained unchanged without any further growth (**Figs. 4 a, b**). Total length of cracks at the time of initiation was 9.45cm and on the 10th and last day was 21.765cm, i.e. 2.3 times of the initial length. The widest spacing along the cracks was 1.1cm. The surface area occupied by the cracks at the time of initiation was 3.632% of 456 cm^2 (total surface area of the sample) which was increased to 10.169%. Only one polygon was formed in the entire experiment period.

3.2.2 Sample 2 (medium sand):

In this sample cracks appeared on the 5thday. Sets of parallel cracks were formed with straighter paths and smoother walls in comparison to those in sample 1. In each of these sets one crack was formed initially and the later ones followed the orientation of the first one. Initially with the appearance of the cracks, four triple junctions were visible and the number was finally increased to nine (**Figs. 3b and 5**). Amongst these nine triple junctions, seven were more prominent than the remaining two and had 120° mutual angular relations between the member cracks. The other two junctions were relatively ill-developed with comparatively much narrower cracks merging at T-junctions (cf. Goehring 2010). It was observed that cracks widened and lengthened with time, i.e. with drying of the sample, intersecting one another to form new triple junctions. The sum of the length of cracks on the initial day of crack formation was 9.92cm and at the end of the experiment was 28.50cm, i.e. almost 2.8 times increase in length. However, the increase in crack length did not result in the formation of any polygons. The widest spacing along cracks was 1.4cm. From the day of first appearance of the cracks to the end of the experiment after ten days the surface area occupied by cracks was 4.27% and 13.13% respectively of total sample surface area.

3.2.3 Sample 3 (grain-size ≤ fine sand):

Cracks first appeared on the 4th day after watering. Extremely smooth walled straight cracks were developed. The number of cracks was much less than that in the two coarser samples. On the 4th day, three triple junctions were formed, of which two were T-junctions (**Fig. 6a**). On the 10th and final day four more triple junctions were developed; out of these (**Fig. 6b**), two had 120° mutual angular relations. One of the younger triple junctions, with arms at 120°, was formed due to emergence of two cracks while others were due to merging of cracks. No polygon was formed. The sum of length of cracks at the day of appearance was 13.379cm and at the tenth or final day of experiment it was 16.687cm, i.e. only about 1.2 times increase. The widest spacing along cracks was 1.8cm, which was wider than the other two sieved samples. At first appearance of cracks, 3.61% of surface area was occupied by cracks and at the end it was 13.02%.

3.3 Comparison of Crack patterns developed in different samples:

Amongst the three samples initiation of crack generation was fastest in the fine grained sample (Sample 3), while in coarsest sample (Sample 1) it is slowest (**Fig. 7**). These results, therefore indicate that while the presence of grains in a wide size range (here Sample 3 consisting of fine sand and finer particles) generally facilitates crack generation in soil, in this experiment the medium sand showed the highest rate of crack growth. In the coarse-grain sample 1(**Fig. 4a**) soil crack-propagation path is more undulated than in the fine–grain sample 3(**Figs. 6a**). The spacing between crack walls widens with decrease in grain-size (**Figs. 4b** and **6b**). In finer soil cracks generated have smoother walls (**Fig. 6b**). The number of triple junctions increases with grain-size (See **Figs. 6a** and **4a**). However uncontrolled variation in grain-size of the soil may give rise to more triple junctions of cracks than found in unmixed samples. In coarser grain samples angular relations of triple junction are 120° while in fine sample T-junctions are more frequent. In fine sand sample triple junctions are fewer in number (See **Figs. 4b** and **6b**). The number of poorly developed cracks is greater in medium sand (sample 2) compared to those found in coarse or fine sand. Younger small cracks mostly follow the orientation of adjacent larger cracks (See **Figs. 3b** and **5**). The finer the grain-size, the lesser is the number of crack-bound polygons (**Fig. 6b**). Delamination cracks were developed only in the sample 3 i.e. fine sample (**Fig. 6b**).

4. Discussion

The XRD results support that the drying and pulverisation procedures were effective, as montmorillonite occurred in samples 2 and 3 but not in 1, whereas polylithionite was identified only in sample 2 and lavendulan only in sample 3. These data thus suggest that fine fractions did not form conglomerations during preparation

before sieving took place. The coarsest sample, fine gravel to coarse sand, showed only quartz but must have contained enough clays/micas to allow cracking, but with these fine fractions effectively below the detection limit during X-ray diffractometry. The mica group component (polylithionite) was presumably comprised mainly of medium sized grains, which survived the river regime before deposition of the soils. Lavendulan, a copper arsenate mineral, is a relatively common contaminant of the groundwater in West Bengal and the Ganga-Brahmaputra River system in general, being sourced most likely from the Himalayan hill ranges (Shah, 2010). It is presumably associated with the fine clay fraction (montmorillonite) found in the finest sample, sample 3, whereas montmorillonite in the medium sands of sample 2 was associated with higher energy levels during deposition, effectively preventing deposition from groundwater in the fine clays.

Evaporation of water from wet sediment leads to generation of cracks (Adams and Hanks 1964; Kodikara et al. 2000; Reineck and Singh 2012). Evaporation from soil depends upon many parameters, like surface of exposure, temperature, humidity, porosity and permeability of soil (Kindle 1917). Water entrapped in sediment evaporates through specific routes which are determined by presence of weak planes. Therefore, these routes may vary according to compaction of soil, sorting of grain-sizes, association of soil grains after inundation. Experiments were performed under similar temperature-humidity conditions, the dimensions of every tray was similar and therefore surface of exposure was the same. The only difference between the samples was the size ranges of constituent grains which in turn exerted its control on differences in permeability and compaction in the relevant sample. Therefore, in different soil samples different kinds of crack patterns evolved though they share the same origin, namely evaporation. After watering, the soil goes through some changes. Water in pore spaces leads to resettlement of particles and organization of invisible water evaporation routes. During the incubation period (time between watering and the first crack appearance) invisible evaporation routes grow wider and deeper and finally become visible as crack patterns after critical evaporation. Resettlement of particles produces numerous invisible weak planes; networks of these planes generate water escape routes and through these routes water gets evaporated. The exposed crack pattern is possibly the manifestation of these water escape routes. With prolonged desiccation, cracks grow wider, longer and deeper.

In the fine sand sample (sample 3), the number of cracks was the least among all three samples, but crack-spacing was the widest. In the coarse sand sample (sample 1), the number of cracks was greater than that in the fine sand and medium sand samples, but with narrower spacing. Inter-granular void space is the least in the fine sand, a condition facilitating shrinkage. The more material shrinks, the greater is the spacing of the cracks (**Fig. 8**). When water is evaporated from sediment pore space, particles tend to collapse into the pore space, resulting

in shrinkage (See **Fig. 8**) (cf. Adams and Hanks 1964; Colina and Roux 2000; Shorlin 2000). Shrinkage is greatest in fine-sand, causing it to yield wider crack-spacing than the other samples. In the case of medium sand, shrinkage and crack spacing were intermediate. Shrinkage makes the sample compacted preventing linear growth (Stoltz et al. 2012). This is the reason behind the increase in the number of cracks with increase in grain-size of the sample. After appearance of cracks they acted as air passages to the deeper part of the samples favouring further evaporation and shrinkage and new crack formation.

It is quite obvious that smoothness of crack walls depends on grain-size of the sample. Desiccation leads to compaction of soil by bringing particles closer to each other and destroying inter-granular voids. The smaller the inter-granular void spaces are, the less is the curvature of the crack. This also explains the smooth crack walls found in the finer samples, distinct from the coarser samples. The randomness of the crack orientations accelerates merging of one crack into another. It is a property of cracks that they propagate towards other cracks (cf., Goehring 2010). Therefore, only the coarser grain-sized sample had a polygon formed by cracks and the finer two samples did not.

Desiccation leads to shrinkage, where cohesion between grains creates tension; when tension exceeds soil shear strength, a crack develops, and in order to reduce tension cracks would tend to remain close to each other (Weinberger 1999).

Greater permeability of coarse samples (Pettijohn, 1975; Todd and Mays, 2004) possibly enhances drying and desiccation by allowing more air, compared to finer samples, while lesser permeability of fine samples does not allow desiccation of the sample so profusely. This may be the reason behind dominance of 120º triple junctions in coarse grained sample and dominance of T-junction type triple junctions in fine samples.

In fine sand the number of cracks is fewer than in the coarse sand, the crack wall is smooth, and there is lesser opportunity for cracks to bend and merge; additionally, finer sand produces greater cohesion that retards cracks to grow further. This much larger amount of cohesion directly controls polygon formation.

From the experiment performed in this research, grain-size is shown to have a direct influence on crack formation and the characteristics of the resultant crack patterns. Obviously, sieving which is used to generate the three different size fraction samples, will also directly impact the mineral composition of the sample, as demonstrated in the XRD results with clay and mica components determined only for the fine and medium sand samples. Despite this, more cracks were observed to form in the coarsest sample than in the other two, demonstrating that all three samples contain above the minimum phyllosilicates needed to induce crack

formation. Cracks form in soil through the interaction, both positive and negative, of multiple genetic factors, and the data we present here strongly suggest that grain-size be added to those formative factors.

5. Conclusions

It is evident from experiments that grain-size of the soil is the key factor behind generation and evolution in soil cracks. The following conclusions can be drawn from the experiments.

a. After critical evaporation, cracks are visible to the un-aided eye. Time duration between watering and visible crack pattern is addressed as the incubation period.

b. The finer the sediment, the shorter is the incubation period and the faster is the crack formation.

c. The finer the sediment, the fewer is the number of polygons formed and the wider is the spacing between the polygons.

d. Crack pattern varies with grain-size and once formed a pattern remains unchanged for the entire cycle (ten days in the case of this experiment)

e. Cracks in finer sediments have smoother walls than those in coarser sediments; the fineness of particles increases with watering.

The comparative study of different grain sizes can reveal a lot about the behaviour of cracks in sand, silt, mud beds.

Acknowledgements

The authors express gratitude to Dr. Sunipa Mandal for the XRD analysis, Dr. Abhijit Chakraborty, and Dr. Sujata Tarafdar, for helpful discussions and advice during research work and preparation of manuscript. Suggestions from the editor and anonymous reviewers have helped to upgrade this paper. The authors are thankful to them.

References

Adams JE, Hanks RJ (1964) Evaporation from Soil Shrinkage Cracks. Soil Science Society of America Journal 28.2(1964):281-284. https://doi:10.2136/sssaj1964.03615995002800020043x.

Baldwin CT (1974) The control of mud crack patterns by small gastropod trails. J Sediment Res 44:695-697.https://doi.org/10.1306/74D72ADB-2B21-11D7-8648000102C1865D.

Biscaye PE (1965) Mineralogy and sedimentation of recent deep-sea clay in the Atlantic Ocean and adjacent seas and oceans. Geological Society of America Bulletin 76:803-832. https://doi.org/10.1130/0016-7606(1965)76[803:MASORD]2.0.CO;2.

Bohn S, Pauchard L, Couder Y (2005) Hierarchical crack pattern as formed by successive domain divisions. Phys Rev E 71(4):046214. https://doi.org/10.1103/PhysRevE.71.046214.

Brown G, Brindley GW (1984) Crystal Structures of Clay Minerals and Their X-ray Identification. Mineralogical Society London.

Colina H, Roux S (2000) Experimental model of cracking induced by drying shrinkage. The European Physical Journal E1(2-3):189-194. https://doi.org/10.1007/s101890050021.

Collinson JD, and Thompson DB (1982) Sedimentary Structures, George Allen and Unwin, London.

Corte A, Higashi A (1960) Experimental research on desiccation cracks in soil. U.S. army Snow Ice and Permafrost Research Establishment, Crops of Engineers, Willmette, Illinois, U.S.A. Research Report No. 66.

Gauthier G, Lazarus V, Pauchard L (2010). Shrinkage star-shaped cracks: Explaining the transition from 90 degrees to 120 degrees. Europhys. Lett. 89(2):26002. https://doi.org/10.1209/0295-5075/89/26002.

Goehring L (2013) Evolving fracture patterns: columnar joints, mud cracks and polygonal terrain. Philosophical Transactions of the Royal Society A: Mathematical, Physical and Engineering Sciences 371(2004):20120353. https://doi.org/10.1098/rsta.2012.0353.

Goehring L, Conroy R, Akhter A, Clegg WJ, Routh AF (2010) Evolution of mud-crack patterns during repeated drying cycles. Soft Matter6(15):3562-3567. https://doi.org/10.1039/B922206E.

Goehring L, Nakahara A, Dutta T, Kitsunezaki S, Tarafdar S (2015) Desiccation cracks and their patterns: Formation and Modelling in Science and Nature. John Wiley & Sons.

Grabowski RC, Droppo IG, Wharton G (2011) Erodibility of cohesive sediment: The importance of sediment properties. Earth-Sci Rev 105(3-4):101-120. https://doi.org/10.1016/j.earscirev.2011.01.008.

Groisman A, Kaplan E (1994) An experimental study of cracking induced by desiccation. EurophysLett25(6):415. https://doi.org/10.1209/0295-5075/25/6/004.

ISO E (2002) 14688-1: 2002: Geotechnical investigation and testing–Identification and classification of soil–Part 1: Identification and description. International Organization for Standardization, Geneva.

Kindle EM (1917) Some factors affecting the development of mud-cracks. JGeol25(2):135-144. journals.uchicago.edu/doi/pdfplus/10.1086/622446.

Kodikara JK, Barbour SL, Fredlund DG (2000) Desiccation cracking of soil layers. Unsaturated soils for Asia 90(5809):139.

Korneta W, Mendiratta SK, Menteiro J (1998) Topological and geometrical properties of crack patterns produced by the thermal shock in ceramics. Physical Review E 57(3):3142. https://doi.org/10.1103/PhysRevE.57.3142.

Liang J, Huang R, Prevost JH, Suo Z (2003) Evolving crack patterns in thin films with the extended finite element method. Int J Solids Struct 40(10):2343-2354. https://doi.org/10.1016/S0020-7683(03)00095-7.

Nichols G (2009) Sedimentology and stratigraphy. John Wiley & Sons.

Partheniades E (2009) Cohesive sediments in open channels: erosion, transport and deposition. Butterworth-Heinemann.

Peron H, Hueckel T, Laloui L, Hu L (2009) Fundamentals of desiccation cracking of fine-grained soils: experimental characterisation and mechanisms identification. Canadian Geotechnical Journal 46(10):1177-1201. https://doi.org/10.1139/T09-054.

Pettijohn FJ (1975) Sedimentary rocks (Vol. 3). New York: Harper & Row.

Reineck HE, Singh IB (2012) Depositional sedimentary environments: with reference to terrigenousclastics. Springer Science & Business Media.

Schieber J (1998) Possible indicators of microbial mat deposits in shales and sandstones: examples from the Mid-Proterozoic Belt Supergroup, Montana, USA. Sediment Geol 120:105-124. https://doi.org/10.1016/S0037-0738(98)00029-3.

Schieber J, Bose PK, Eriksson PG, Banerjee S, Sarkar S, Altermann W, Catuneanu O (2007) Atlas of microbial mat features preserved within the siliciclastic rock record. Elsevier, Amsterdam, Atla in Geosc 2:311.

Shah BA (2010) Arsenic-contaminated groundwater in Holocene sediments from parts of Middle Ganga Plain, Uttar Pradesh, India. CurrSci 98/10:1359-1365.

Shorlin KA, de Bruyn JR, Graham M, Morris SW (2000) Development and geometry of isotropic and directional shrinkage-crack patterns. Physical Review E 61(6):6950. https://doi.org/10.1103/PhysRevE.61.6950.

Stoltz G, Cuisinier O, Masrouri F (2012) Multi-scale analysis of the swelling and shrinkage of a lime-treated expansive clayey soil. Applied Clay Science 61:44-51. https://doi.org/10.1016/j.clay.2012.04.001.

Style RW, Peppin SS, Cocks AC (2011) Mud peeling and horizontal crack formation in drying clays. J Geophys 116:(F1). https://doi.org/10.1029/2010JF001842.

Tan KH (2005) Soil sampling, preparation, and analysis. CRC press.

Todd DK, Mays LW (2004) Groundwater hydrology. John Wiley & Sons.

Vogel HJ, Hoffmann H, Roth K (2005) Studies of crack dynamics in clay soil: I. Experimental methods, results, and morphological quantification. Geoderma 125(3-4):203-211. https://doi.org/10.1016/j.geoderma.2004.07.009.

Weinberger R (1999) Initiation and growth of cracks during desiccation of stratified muddy sediments. J StructGeol 21(4):379-386. https://doi.org/10.1016/S0191-8141(99)00029-2.

Zabat M, Vayer-Besançon M, Harba R, Bonnamy S, Van Damme H (1997) Surface topography and mechanical properties of smectite films. Trends in Colloid and Interface Science XI Steinkopff:96-102. https://doi.org/10.1007/BFb0110970.

Figure caption:

Fig. 1: (**a)** Photograph of prepared sample 1, on the first day of the cycle; (**b)** Photograph of prepared sample 2, on the first day of the cycle; (**c)** Photograph of prepared sample 3, on the first day of the cycle.

Fig. 2: (**a)** XRD analysis of sample 1; (**b)** XRD analysis of sample 2; (**c)** XRD analysis of sample 3.

Fig. 3: (**a)** Photograph of sample 2, after inundation. Pore throats are shown in rectangular boxes; (**b**) Photograph of sample 2, on the first appearance of crack pattern, depicting triple junctions (in rectangular boxes) originated from pore throats.

Fig. 4: (**a)** Photograph of sample 1, on the first appearance of crack pattern, the triple junctions are shown in rectangular boxes; (**b)** Photograph of fully developed crack pattern in sample 1, ill developed cracks are within the rectangular boxes.

Fig. 5: Photograph of fully developed crack pattern in sample 2, older cracks are in rectangular boxes, later developed parallel cracks are marked by arrows.

Fig. 6: (**a)** Photograph of sample 3, on the first appearance of crack pattern (existing triple junctions and newly appearing cracks are in rectangular boxes); (**b**) Photograph of fully developed crack pattern in sample 3, merged cracks are in rectangular boxes.

Fig. 7: Percentage of area cracked in every cycle with respect to time.

Fig. 8: Schematic diagram of crack generation with respect to shrinkage. Drawn from Fig. 4b.

Table caption:

Table 1: Water added (in millilitre) to each sample to attain saturation.

Figure 1a

Figure 1b

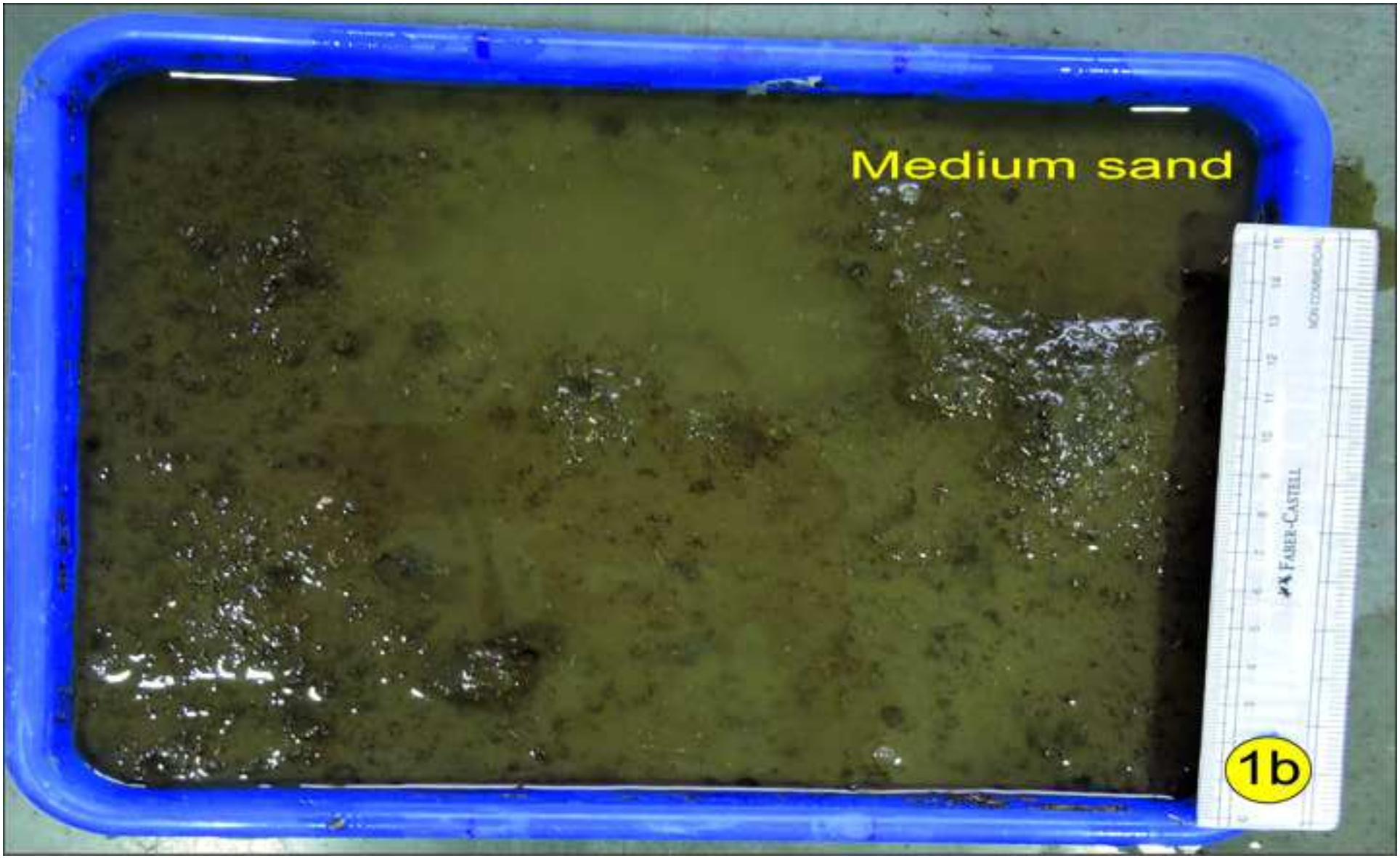

Figure 1c

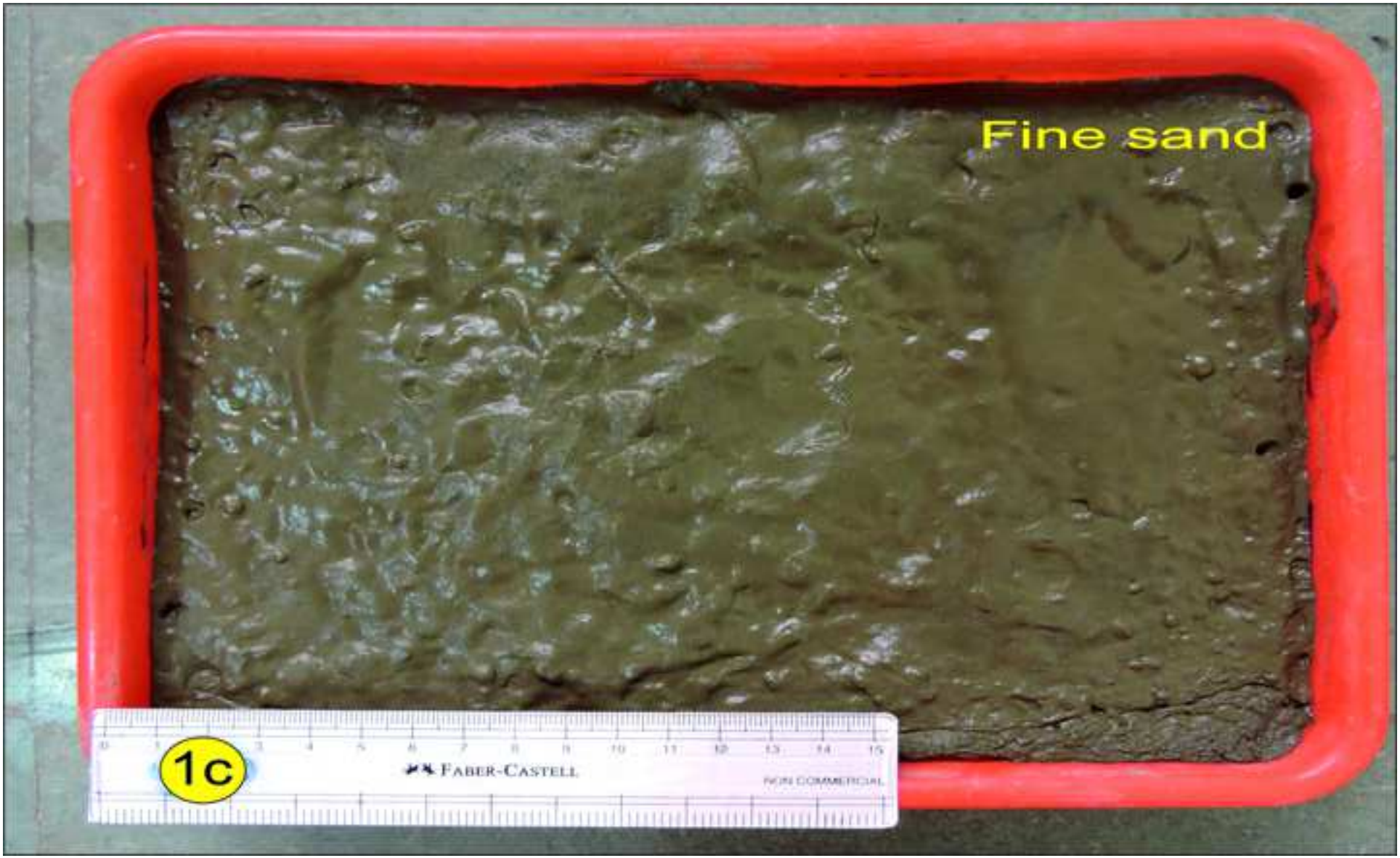

Figure 2a

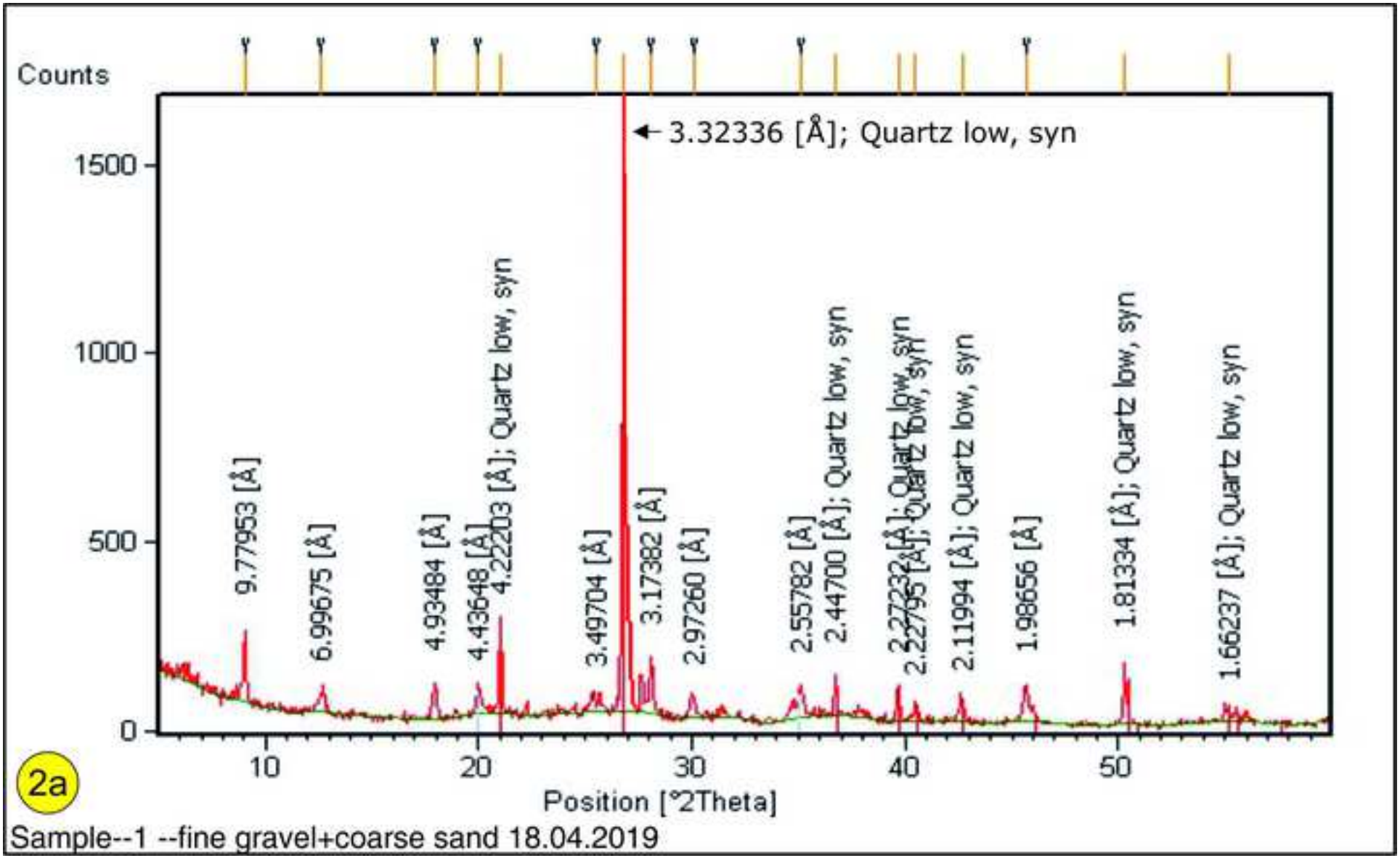
Counts
3.32336 [Å]; Quartz low, syn
1500
1000
500
0
9.77953 [Å]
6.99675 [Å]
4.93484 [Å]
4.43648 [Å]
4.22203 [Å]; Quartz low, syn
3.49704 [Å]
3.17382 [Å]
2.97260 [Å]
2.55782 [Å]
2.44700 [Å]; Quartz low, syn
2.27232 [Å]; Quartz low, syn
2.22795 [Å]; Quartz low, syn
2.11994 [Å]; Quartz low, syn
1.98656 [Å]
1.81334 [Å]; Quartz low, syn
1.66237 [Å]; Quartz low, syn
10
20
30
40
50
Position [°2Theta]
2a
Sample--1 --fine gravel+coarse sand 18.04.2019

Figure 2b

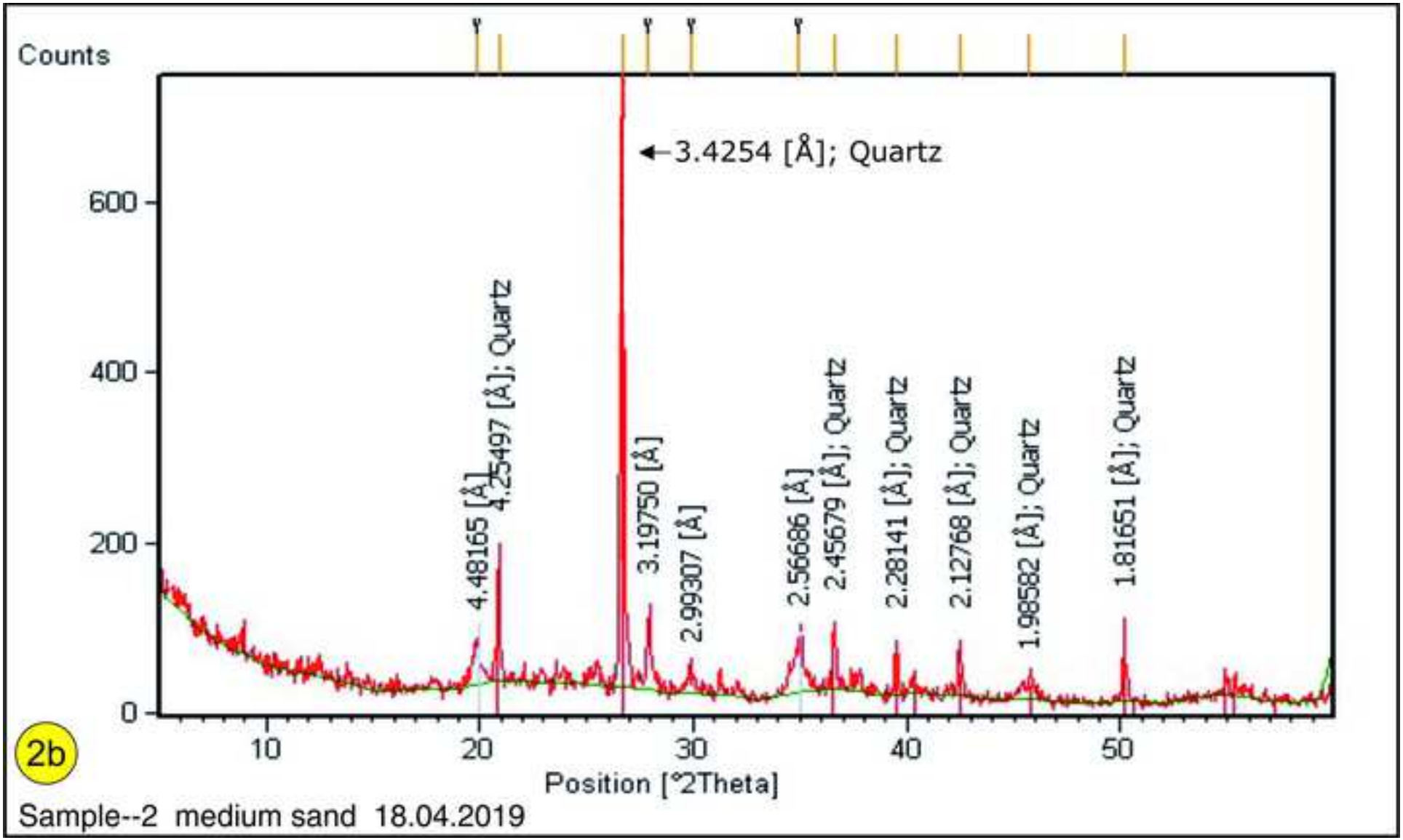
Counts
3.4254 [Å]; Quartz
4.48165 [Å]
4.25497 [Å]; Quartz
3.19750 [Å]
2.99307 [Å]
2.56686 [Å]
2.45679 [Å]; Quartz
2.28141 [Å]; Quartz
2.12768 [Å]; Quartz
1.98582 [Å]; Quartz
1.81651 [Å]; Quartz
600
400
200
0
10
20
30
40
50
Position [°2Theta]
2b
Sample--2 medium sand 18.04.2019

Figure 2c

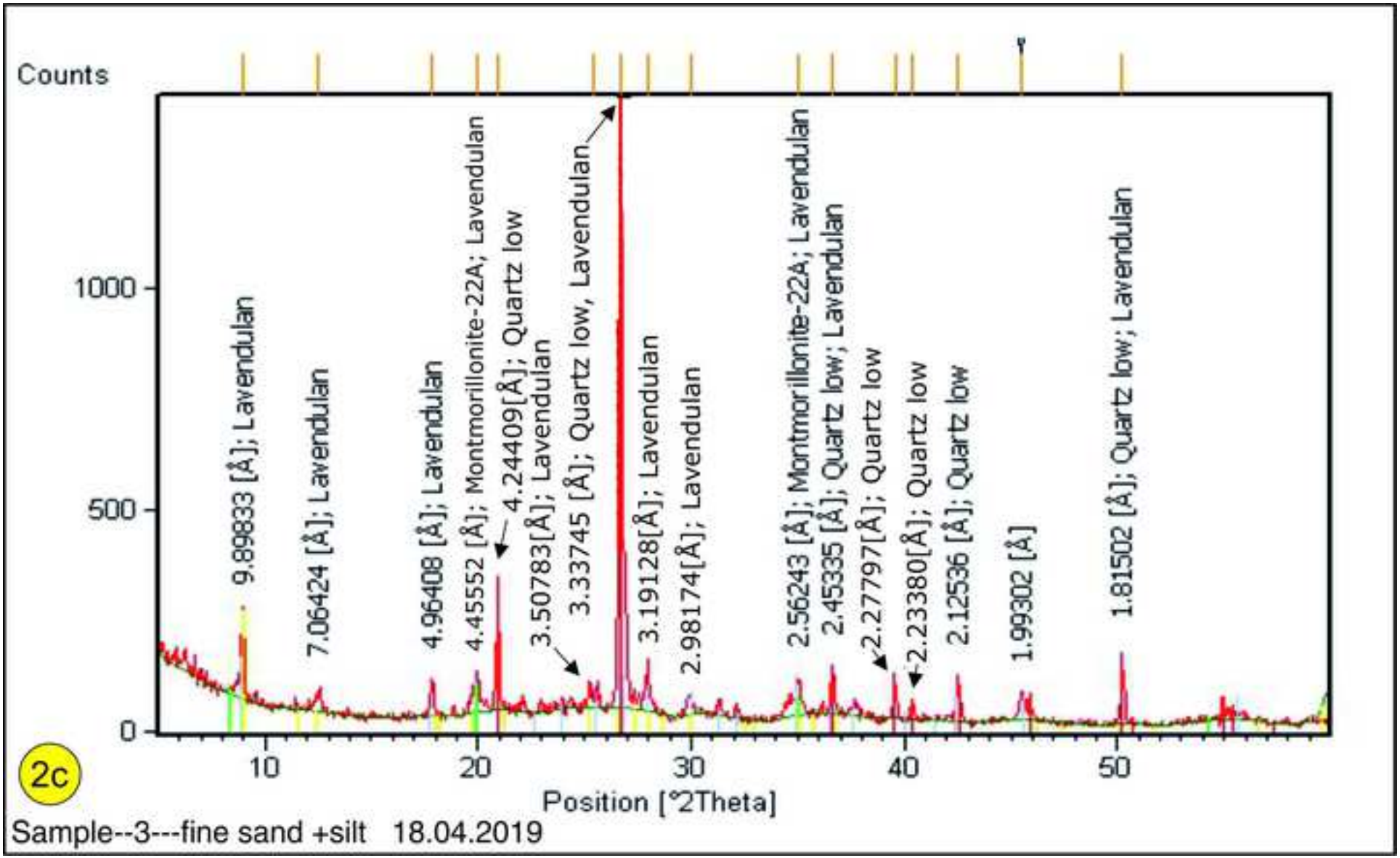
Counts
1000
500
0
9.89833 [Å]; Lavendulan
7.06424 [Å]; Lavendulan
4.96408 [Å]; Lavendulan
4.45552 [Å]; Montmorillonite-22A; Lavendulan
4.24409[Å]; Quartz low
3.50783[Å]; Lavendulan
3.33745 [Å]; Quartz low, Lavendulan
3.19128[Å]; Lavendulan
2.98174[Å]; Lavendulan
2.56243 [Å]; Montmorillonite-22A; Lavendulan
2.45335 [Å]; Quartz low; Lavendulan
2.27797[Å]; Quartz low
2.23380[Å]; Quartz low
2.12536 [Å]; Quartz low
1.99302 [Å]
1.81502 [Å]; Quartz low; Lavendulan
10
20
30
40
50
Position [°2Theta]
2c
Sample--3---fine sand +silt 18.04.2019

Figure 3a

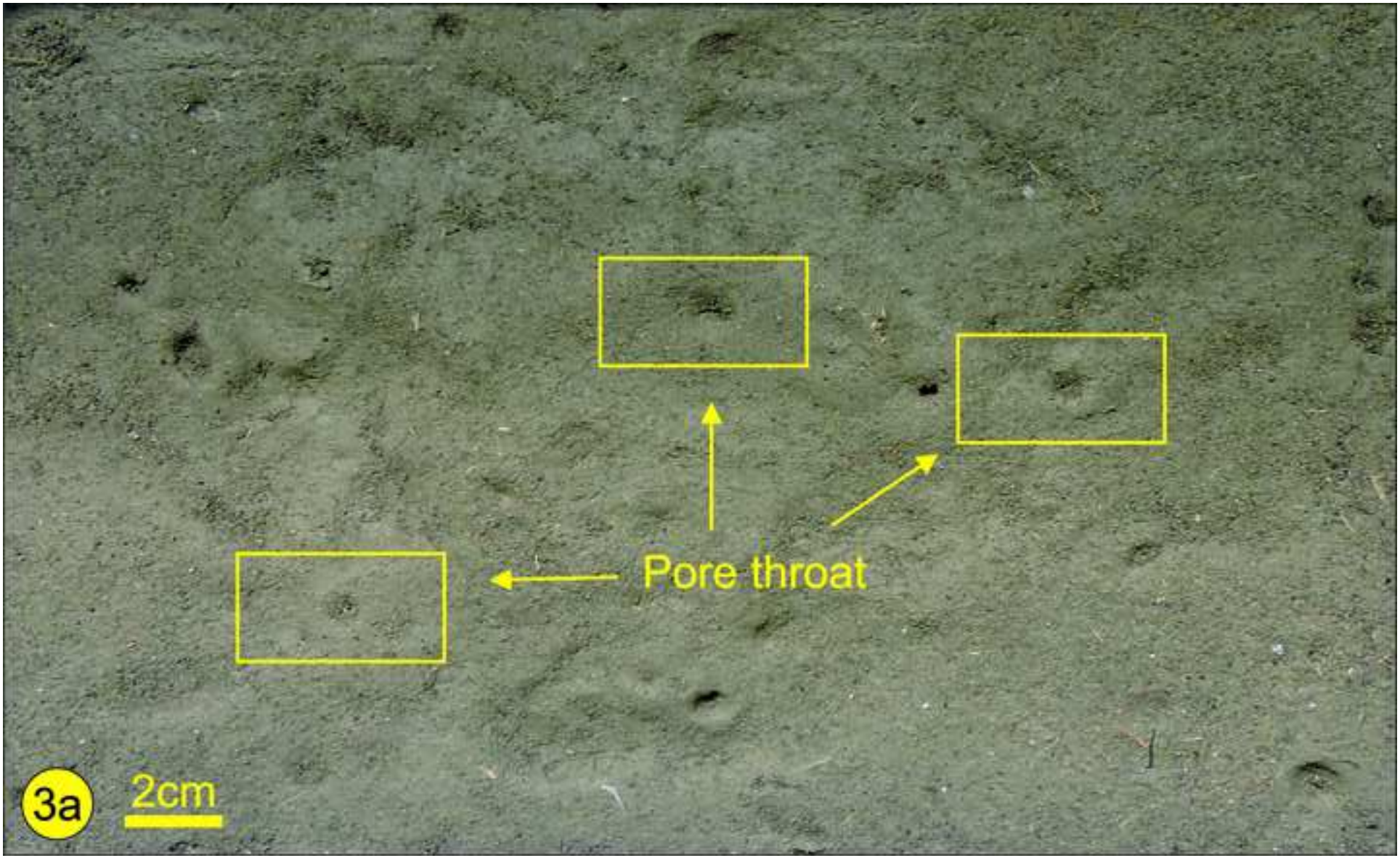

Figure 3b

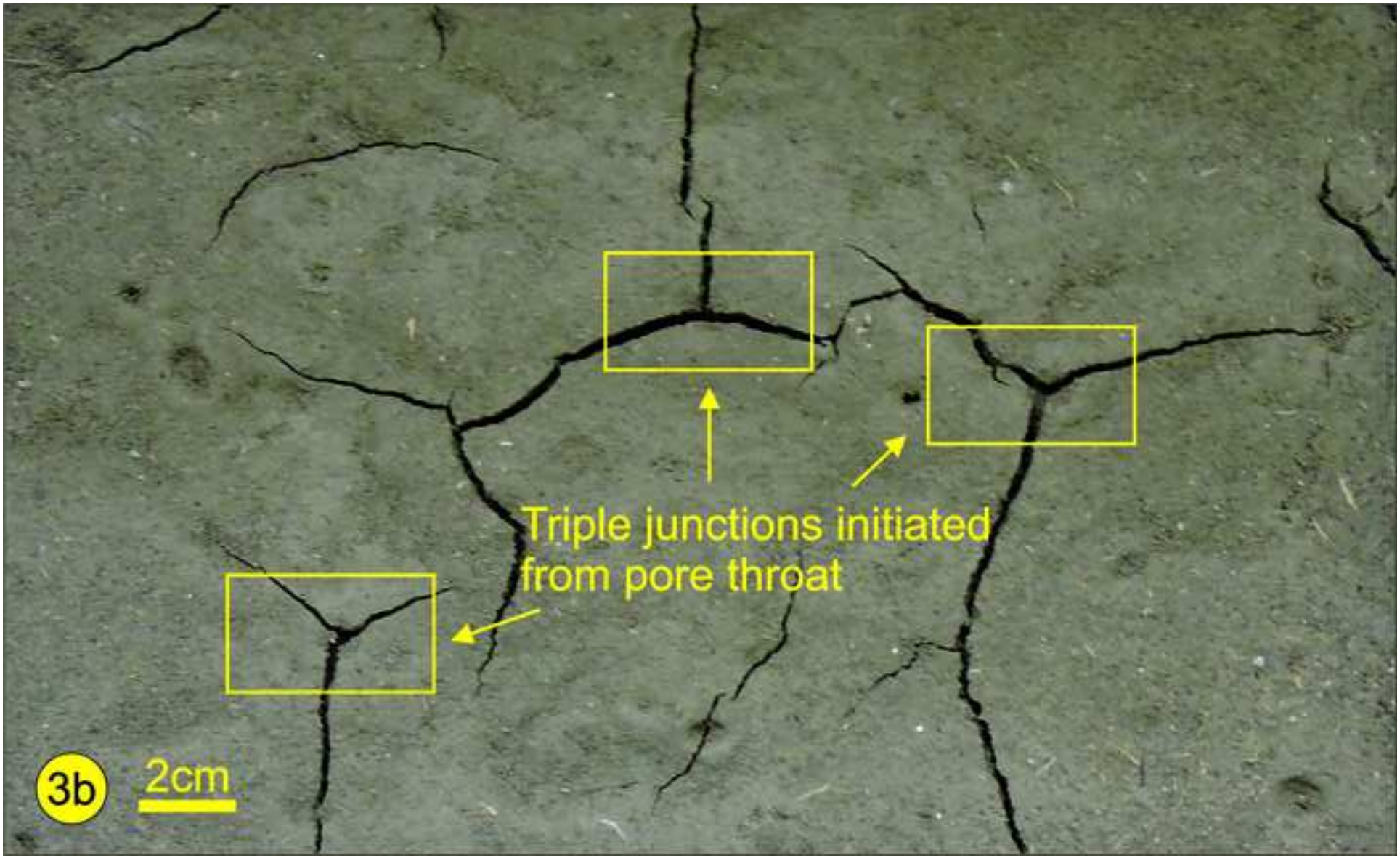

Figure 4a

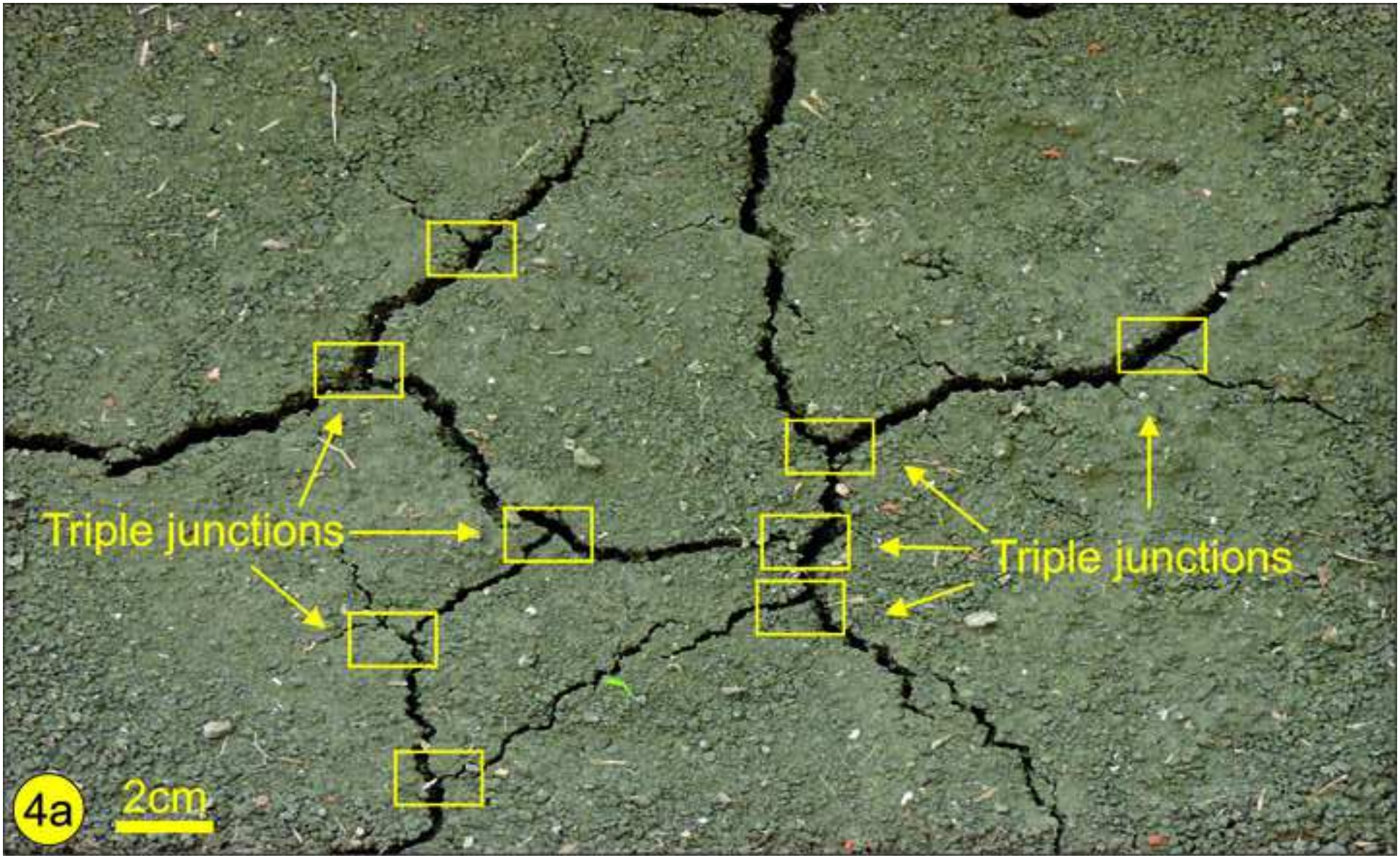

Figure 4b

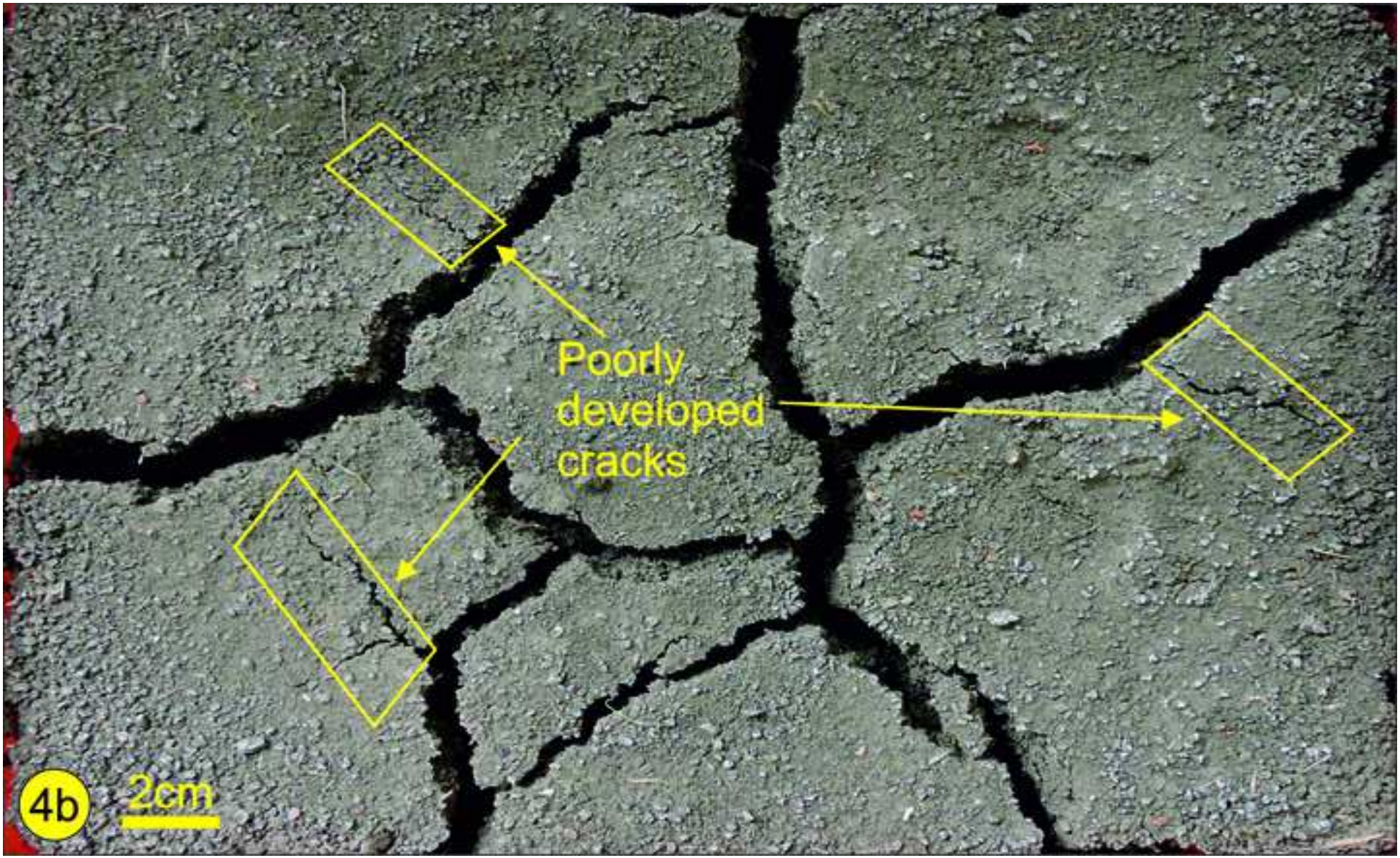

Figure 5

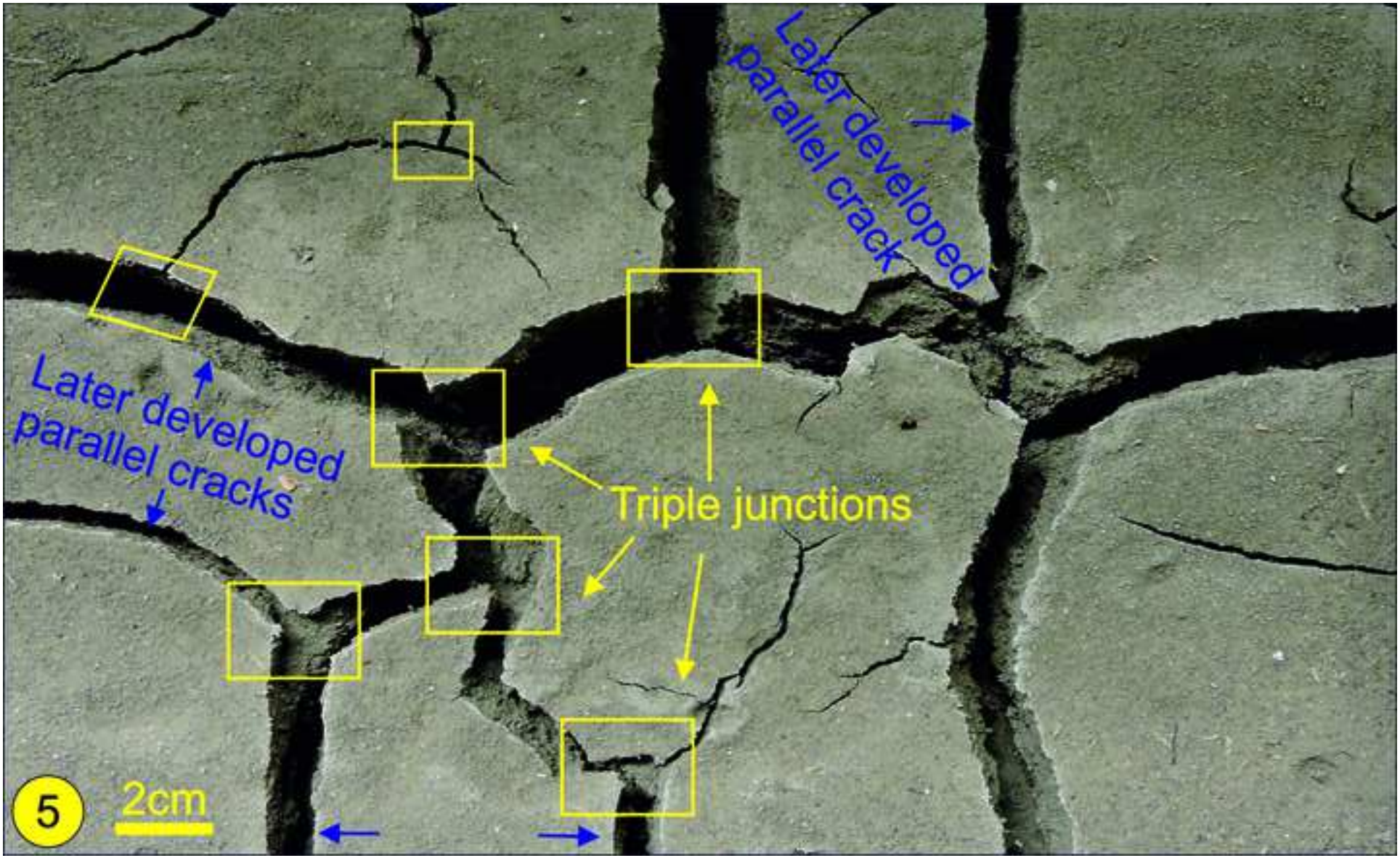
Later developed parallel crack
Later developed parallel cracks
Triple junctions
5
2cm